Antifungal nanosuspensions with surfactants and silver for the treatment of onychomycosis

European Journal of Pharmaceutics and Biopharmaceutics 179 (2022) 194–205

Contents lists available at ScienceDirect

European Journal of Pharmaceutics and Biopharmaceutics

journal homepage: www.elsevier.com/locate/ejpb

Antifungal nanosuspensions with surfactants and silver for the treatment of onychomycosis

Hisham Al-Obaidi [a,*], Ieva Petraityte [a], Thomas Hibbard [a], Mridul Majumder [b], Rachith Kalgudi [c], Mohammed Gulrez Zariwala [c]

[a] The School of Pharmacy, University of Reading, Reading RG6 6AD, United Kingdom
[b] M2M Pharmaceuticals Ltd, The Gateway Building, 1 Collegiate Square, Thames Valley Science Park (TVSP), Reading RG2 9LH, United Kingdom
[c] Faculty of Science & Technology, University of Westminster, 115 New Cavendish Street, London W1W 6UW, United Kingdom

ARTICLE INFO

Keywords:
Fungal biofilms
Nanosuspensions
Solid dispersions
Nail infections
Saturation solubility
Silver nanoparticles

ABSTRACT

Fungal nail infection (Onychomycosis) often requires prolonged treatment and is associated with a high risk of resistance to treatment. Here in this contribution, we introduce a novel approach to enhance penetration and antifungal activity of the antifungal drug griseofulvin (GF). Solid dispersions were prepared with hydroxypropyl methylcellulose acetate succinate (HPMCAS) and combined with surfactant (either sodium dodecyl sulphate (SDS), dodecyl trimethylammonium bromide (DTAB), or Pluronic F127) using mechanochemical activation. The prepared powders were then suspended with spray-dried silica-coated silver nanoparticles and applied onto infected bovine hooves to assess permeability and antifungal activity. The results showed that the prepared nanosuspensions significantly suppressed fungal activity causing disruption of fungal biofilms. Raman mapping showed enhanced permeation while dynamic vapor sorption (DVS), and particle size measurements showed varied effects depending on the type of surfactant and milling conditions. The prepared nanosuspensions displayed enhanced solubility of the poorly soluble drug reaching approximately 1.2 mg/mL. The results showed that the dispersions that contained DTAB displayed maximum efficacy while the inclusion of colloidal silver did not seem to significantly improve the antifungal activity compared to other formulations.

1. Introduction

Onychomycosis is a fungal infection of the human nail that is commonly caused by dermatophytes, yeasts and non-dermatophytic moulds [1]. A significant number of the global population is affected by onychomycosis causing considerable impact on the quality of life of many patients [2]. The resistant and chronic nature of onychomycosis has been attributed to the formation of fungal biofilms [3]. Biofilms are surface-associated microbial communities that exist within a self-secreted matrix consisting primarily of polysaccharides, proteins, nucleic acid [4]. Biofilm structures formed by fungi may present favourable conditions for survival in the environment as well as within an infected host [5].

Dermatophytes such as *T. rubrum*, a keratinolytic saprophytic fungi, is known to form biofilms and is commonly implicated as a cause for fungal infection of the nails (onychomycosis) [6]. Current treatment options for onychomycosis include oral and topical preparations. Unfortunately, oral antifungal therapies are associated with toxic side effects including liver impairment and require caution when used in patients with diabetes, renal impairment, and peripheral arterial disease. Among different antifungal drugs, griseofulvin (GF) has fungistatic effect against *Tricophyton* species, which are the most common cause of onychomycosis. To reach the fungal active site and produce a therapeutic effect, GF must physically adsorb to the surface of the nail. As the human nail is largely composed of keratin, with the aid of appropriate formulation approach, the binding between keratin and griseofulvin can facilitate permeation of the drug into the nail. However, griseofulvin is practically insoluble in aqueous media and achieving high concentrations of the drug at the nail surface will not be possible.

Current topical treatments are based on dissolving the drug in a volatile solvent (typically acetone or ethanol) forming a lacquer. A layer of the drug lacquer is applied on the nail so that allowing the solvent to evaporate leaving a thin film of the drug on the nail. The hurdle of this approach is that the drug will potentially be deposited as crystals that will not be able to penetrate through the keratin network. It may also deprive the nail from its moisture content further restricting drug

* Corresponding author.
E-mail address: h.al-obaidi@reading.ac.uk (H. Al-Obaidi).

https://doi.org/10.1016/j.ejpb.2022.09.004
Received 18 May 2022; Received in revised form 4 August 2022; Accepted 5 September 2022
Available online 10 September 2022

permeability. One potential approach to enhance efficacy is by forming viscous supersaturated solutions/ suspensions of the drugs allowing maximum concentrations reaching the fungal biofilm.

As most of antifungal drugs are highly hydrophobic and neutral molecules; salt formation is not possible to prepare the supersaturated solutions/ suspensions. Thus, the use of solid dispersions to form the supersaturated solutions/ suspensions is an appropriate approach by which the drug is molecularly mixed with a polymer [7,8]. The equilibrium between the undissolved microparticles will maintain high solubility and prevents recrystallization of the drug. We have shown before GF solid dispersions with hypromellose acetate succinate (HPMCAS) remain stable against recrystallization [9]; hence HPMCAS can be used to prevent recrystallization of GF as well as to optimize adherence to the nail surface. Recently, we have shown possible positive role of surfactants when incorporated in spray dried solid dispersions enhancing miscibility between the drug and the polymer [10]. A previous study examined the possible detachment of biofilms via the inclusion of the anionic sodium dodecyl sulphate (SDS) and the cationic cetyltrimethyl ammonium bromide (CTAB) [11]. The study showed that increasing the concentration of the surfactants (SDS) promoted significant inactivation of the biofilms.

There are various reports that showed the potential use of silver nanoparticles as antifungal agents [12,13] and in particular against dermatophytes [14–16]. Hence, the aim of this study is to formulate a nanosuspension containing surfactant based polymeric dispersion doped with the antifungal drug griseofulvin (GF)/ silver nanoparticles and test its efficacy against *T. rubrum* biofilms. The prepared particles were assessed using dynamic vapour sorption (DVS) for water uptake and stability, Raman mapping to assess permeation, solubility, and particle size measurements of the nanosuspensions. Griseofulvin is the first line treatment for tinea pedis and tinea corporis infections hence we use it here to study its potential application combined with surfactants to damage fungal biofilms. Three different surfactants were used which are anionic sodium dodecyl sulphate (SDS), cationic dodecyletrimethylammonium bromide (DTAB) and non-ionic pluronic (F127). Apart from the obvious difference in terms of the charge, it was shown recently that anionic surfactants had a notable effect on the binding of GF to the polymer polyethylene glycol [17]. This is possibly due to the counterions forming a link between the polymer and the aggregation of anionic surfactant with GF. This effect may not be seen with a non-ionic surfactant, and to a small extent for cationic surfactants [17]. Hence, such interactions could play a key role in disruption of the biofilm network with the aid of surfactant and the drug.

2. Materials and methods

2.1. Materials

Griseofulvin (GF), silver nanopowder (<100 nm), sodium dodecyl sulphate (SDS, molecular weight 288.37 $gmol^{-1}$), dodecyltrimethylammonium bromide (DTAB, molecular weight 308.3 $gmol^{-1}$) and Pluronic F127 (average molecular weight 12,600 $gmol^{-1}$) were purchased from Sigma Aldrich (UK). Hydroxypropylmethylcellulose acetate succinate (HPMCAS, average MW 20,000 Da) was obtained from Shin-Etsu (Japan).

2.2. Preparation of solid dispersions and nanosuspensions by ball milling and spray drying

Solid dispersions of GF, HPMCAS (1:1 w/w) and surfactant (SDS 1 %, 2.5 % and 5 %, Pluronic F-127 1 %, 2.5 % and 5 % or DTAB 1 %, 2.5 % and 5 %) (total mass of 1 g) were prepared by ball milling the mixtures in a zirconium oxide lined grinding jars containing one zirconium ball of a diameter of 12 mm using a Retsch MM200 mill (Castleford, UK). The samples were ball milled at a frequency of 30 s^{-1} for 2, 4, 6, 8, 10 and 15 min with 2 min cooling time after every 2 min of milling to avoid overheating of the mill. This was followed by a suspension stage by which the powder was suspended in deionised water using bath sonication to form 1 % w/v nanosuspensions. stability of the suspensions was evaluated using particles size measurements as explained below. The nanosuspensions were always made fresh to avoid inconsistency. Physical mixtures (total weight 1 g) composed of a 1:1 wt ratio of GF and HPMCAS, with and without 1, 2.5 or 5 wt% surfactant (either SDS, DTAB or Pluronic F127) were prepared by trituration in a pestle and mortar for 10 min. Prior to the grinding all components were sieved using 120 μm sieve to prevent agglomeration and ensure consistency among prepared samples. To prepare the silver containing particles, the particles were first coated with silica using same process described previously [18]. The particles were then spray dried using a Mini spray dryer B-290 from Büchi (Laboretechnik AG Switzerland) and nitrogen gas was used as the drying gas. The formed silica coated silver nanopowders were then physically mixed with the solid dispersions particles that were prepared by ball milling and suspended. The ratio of silver was maintained in all dispersions at 0.01 % w/w. Details of all prepared formulations are summarised in Table 1.

2.3. Particle size analysis

Particle size of the nanosuspensions was determined using laser diffraction (Malvern Instruments, Mastersizer, UK). Around 10mg of formulation was accurately weighed and dispersed in a buffer (pH 6.8) which was prepared by dissolving 0.9 g of sodium hydroxide and 6.9 g of sodium dihydrogen orthophosphate into 1 L of distilled water. The pH of a prepared buffer solution was confirmed using a pH meter. Each sample was measured in triplicate and the particle size was expressed as the volume or mass moment mean diameter, D [4,3].

2.4. Differential scanning calorimetry

Differential scanning calorimetry (DSC) experiments were performed using DSC Q2000 (TA instruments, UK). Around 10 mg of solid dispersion was loaded into an aluminium pan which was hermetically sealed and a pin hole made in the lid to allow the removal of any residual moisture. The pan was then heated to 90 °C where they were held for 10 min in order to remove any moisture present in the sample, after which time they were cooled to 25 °C, where they were equilibrated for 5 min, prior to heating to 250 °C at a rate of 10 °C/min. The melting point, heat of fusion and heat of crystallisation (in J/g) of the samples were determined with the heat of fusion being calculated based on the melting endotherm of the pure crystalline drug. Each sample was measured in triplicate.

2.5. Solubility studies

The apparent saturation solubility of GF was determined by

Table 1
Summary of prepared formulations, all formulations were suspended in deionised water to form the nanosuspensions.

Formulation	Composition
F1	GF (49.5 %): HPMCAS (49.5 %) + 1 % Ag
F2	GF (47 %): HPMCAS (47 %) + 1 % Ag + 5 % SDS
F3	GF (47 %): HPMCAS (47 %) + 1 % Ag + 5 % DTAB
F4	GF (47 %): HPMCAS (47 %) + 1 % Ag + 5 % Pluronic F127
F5	GF (47.5 %): HPMCAS (47.5 %) + 5 % SDS
F6	GF (47.5 %): HPMCAS (47.5 %) + 5 % DTAB
F7	GF (47.5 %): HPMCAS (47.5 %) + 5 % PluronicF127
F8	GF (48.75 %): HPMCAS (48.75 %) + 2.5 % SDS
F9	GF (48.75 %): HPMCAS (48.75 %) + 2.5 % DTAB
F10	GF (48.75 %): HPMCAS (48.75 %) + 2.5 % PluronicF127
F11	GF (49.5 %): HPMCAS (49.5 %) + 1 % SDS
F12	GF (49.5 %): HPMCAS (49.5 %) + 1 % DTAB
F13	GF (49.5 %): HPMCAS (49.5 %) + 1 % PluronicF127

accurately weighing approximately 20 mg of solid dispersion and making up to 1 mL with phosphate buffer solution (pH 6.8). The resulting dispersion was mixed at 20 ± 2 °C for 72 h using rota-mixer (Bibby Scientific Limited, UK), after which time the sample was centrifuged for 20 min at 13,000 rpm (Heraeus Biofuge Pico centrifuge). Three aliquots of the supernatant were then removed and diluted with buffer solution (pH 6.8) to enable quantification of the amount of griseofulvin using UV/Vis spectrometry at $\lambda^{max} = 294$ (PerkinElmer Lambda 2). Each sample was measured in triplicate and the mean value ± SD were calculated.

2.6. Characterization of solid dispersions by X-ray powder diffraction

A thin layer of the sample powder was placed on the sample holder. The X-ray powder diffraction (XRPD) spectra of the various samples was determined using a Philips PW3710 X-ray powder diffractometer using CuK radiation (30 mA and 45 kV). The samples were analysed using DFFRAC plus XRD commander software (Bruker AXS GmbH, Germany) with a 2θ range of 5-45°, a step size of 0.021064112° and time per step of 1.33 s.

2.7. Dynamic vapour sorption (DVS)

Solid dispersions of GF were weighed at 25 °C using a Dynamic Vapor Sorption analyser (SMS, UK). Two sources of nitrogen gas were used where one of them is a dry gas while the second is 100 % moist. By mixing both of them, the desirable relative humidity was obtained. The variation in weight was recorded using a two-arm balance where the reference pan was empty and the sample pan was filled with the sample. Nitrogen gas was passed over the sample to remove the residual solvent content (using 0 % relative humidity). Once this was achieved, nitrogen gas is passed with the desired relative humidity (RH).

2.8. Raman mapping

Bovine hooves from freshly slaughtered cattle, free of adhering connective and cartilaginous tissue, were soaked in water for 24 hr. As these hooves were a by-product in proper food production and animals were not bred, kept, or sacrificed for scientific purposes but for food production only, ethics committee approval was not required. Membranes of approximately 300 μm thick were then cut from the distal part of the ball horn with a cryotome. Formulations equivalent to 10 mg of GF were suspended in 1 mL of deionised water and each placed in an Eppendorf tube. Bovine hoof samples were cut to size and added to the Eppendorf tubes so that the hoof was completely submerged in the suspension. Samples were left to soak for 24 h and gently spun to reduce sedimentation of suspensions. A hoof sample submerged in 10 mg of GF dissolved in 1 mL of ethanol was used as a control. After 24 h, hoof samples were removed and wiped clean then left to dry. Raman mapping measurements were performed on the hoof samples using a Renishaw inVia Dispersive Raman Microscope equipped with enhanced CCD array detector. Spectra were collected using a 785 nm diode laser at 50 % power from a 3 s accumulation in the 700 – 1800 cm^{-1} spectral range. An area of 50 μm × 100 μm was mapped using a step size of 5 μm and repeat maps were collected in different locations as a uniformity control ($n > 3$). Wire software was used to assess presence of GF at each data point on the map by comparing collected spectra to reference spectra. Most notably, the presence and intensity of peaks at ~ 1620 and ~ 1710 cm^{-1} since no peaks are present at these wavelengths for hoof background spectra.

2.9. Preparation of fungal inoculum

T. rubrum NCPF 935 (PHE, UK) inoculum was prepared from initial growth on potato dextrose agar (PDA) (Sigma-Aldrich, UK) as mentioned by Brilhante *et al.*, 2017 with a few modifications. Briefly, 39 g/L of the solids were fully dissolved in 1 L of distilled water and then sterilised at 121 °C for 15 min. The molten agar was poured into petri plates once it had cooled down to ~ 55 °C and allowed to set. A small piece of *T. rubrum* was excised from the stock and placed in the centre of the PDA plates and allowed to grow for a period of 7–10 days at 28 °C for optimal sporulation. The conidia and hyphal fragments were harvested by covering the cultures with 5 mL of sterile 0.9 % saline solution and by passing a sterile swab over the surface of the cultures. The 0.9 % saline solution containing the conidia and hyphal fragments was then collected and allowed to settle for 5 min at 28 °C to sediment the hyphae and separate the conidia. The conidium suspension was then gently aspirated and transferred to fresh sterile tubes and serially diluted to obtain a suspension containing ~ 5×10^6 cfu/ mL. This was based on cell count performed using a haemocytometer. The conidia suspension was then diluted with 0.9 % saline solution to obtain a concentration of ~ 1 x10^6 cfu/ mL for biofilm formation and subsequent experiments.

2.10. Working stock of GF formulations for biofilm assay

GF formulation powders were initially dissolved in DMSO (dimethyl sulfoxide) (Sigma-Aldrich, UK) according to the CLSI broth microdilution protocol (Wayne, 2008) to a concentration of 800 μg/ mL. The formulations were then further diluted in RPMI 1640 medium, buffered to pH 7 with MOPS to obtain the desired concentrations for biofilm formation assay.

2.11. T. rubrum NCPF 935 biofilm formation assay

Biofilm formation by *T. rubrum* NCPF 935 was performed based on the method as mentioned by dos Santos and Dias-Souza, 2017; Costa-Orlandi *et al.*, 2014 with a few modifications. Briefly, 250 μL of the pre-adjusted (~1×10^6 cfu/ mL) conidia suspension was added to 96-well plates as required. The plates were then incubated at 37 °C for 3 h for adhesion of the conidia to the surface of the wells under static conditions. Subsequently, the growth suspension was replaced with pre-sterilised 250 μL of RPMI 1640 (pH 7) medium containing various griseofulvin formulations. The concentration of the formulations used in this study were equivalent to the MIC of griseofulvin against *T. rubrum* (8 μg/ mL) as depicted by Falahati et al., 2018, following CLSI (the clinical and laboratory standards institute guidelines) M38-A2. Biofilm of *T. rubrum* NCPF 935 were grown with and without the addition of the formulation and grown for a period of 96 h at 37 °C prior to carrying out subsequent assays. The assay was repeated in triplicate for each sample.

2.12. Quantification of total biofilm biomass of T. rubrum NCPF 935 biofilm formation by crystal violet staining

Biofilm biomass was assessed using crystal violet staining as mentioned by Branado *et al.*, 2018 with modifications. Briefly, after 96 h of growth, the excess growth medium was gently aspirated and replaced with 0.5 % (w/v) crystal violet solution to the wells in the 96-well microtiter plate as required. The plates were then incubated at room temperature (~25 °C) for 5 min. The plates were then washed gently under running water till all the excess stain was removed. The crystal violet absorbed by the biofilm was extracted using 33 % (v/v) acetic acid solution and transferred to a fresh 96-well plate and the absorbance was measured at 570 nm using a plate reader (FLUOstar Optima, BMG labtech, UK). The assay was repeated in triplicate for each sample.

2.13. Quantification of total polysaccharide in the biofilm form by T. rubrum NCPF 935 by safranin staining

The extracellular matrix of *T. rubrum* NCPF 935 was stained using safranin following the method by Costa-Orlandi *et al.*, 2014; Seidler *et al.*, 2008 with a few modifications. After biofilm formation for 96 h in 96-well plates, the ECM of *T. rubrum* NCPF 935 was stained using 250 μL

of 1 % (w/v) safranin solution and incubated at room temperature for 5 min and gently and thoroughly washed. The optical density was then measured at 492 nm using a plate reader (FLUOstar Optima, BMG labtech, UK).

2.14. Metabolic activity of T. rubrum NCPF 935 by XTT assay

XTT assay was used based on the method described by Costa-Orlandi *et al.*, 2014 with a few modifications. The assay was used in this study to quantify the metabolic activity of the biofilm with and without the presence of the formulations. Stock solutions of XTT (2,3-bis (2-methoxy-4-nitro-5-sulfophenyl)-5- [carbonyl (phenylamino)]–2H-tetrazolium hydroxide) and menadione were prepared, 1 mg/mL in PBS and 1 mM ethanol respectively, and stored at 4 °C. *T. rubrum* NCPF 935 biofilms were grown with and without the presence of three formulations (F6, F8 and F9, see Table 1) that showed the highest biofilm inhibition. Samples were analysed at 3, 8, 24, 48, 72 and 96 h. To the samples, 50 μL of XTT solution was added along with 4 μL of menadione into the 96-well plates and incubated at 37 °C for 3 h. The resulting formation of formazan salts and colorimetric change were measured in a plate reader at 490 nm (FLUOstar Optima, BMG labtech, UK). RPMI 1640 medium, free of biofilm was used as a negative control.

2.15. Protease activity of T. rubrum NCPF 935

Proteolytic activity of *T. rubrum* NCPF 935 was measured from crude extract with and without the presence of formulations. The method used in this study was based on Kadhim, Al-Janabi and Al-Hamadani, 2015 with a few modifications. Briefly, *T. rubrum* NCPF 935 was grown in PDB (potato dextrose broth) (Sigma-Aldrich, UK) at 37 °C in a rotary shaker at 150 rpm for 7 days. Casein from bovine milk (1 % w/v) (Sigma-Aldrich, UK) was used to determine the proteolytic activity. Briefly, to 500 μL of the casein substrate, 500 μL of *T. rubrum* NCPF 935 filtrate treated with and without the formulations was added along with 100 μL of 0.5 M tris-HCL (pH 8) in test tubes. The reaction was carried out at 40 °C for 30 min and stopped by adding 2 mL of 0.67 M trichloro acetic acid (TCA). The test tubes were allowed to rest at room temperature for 1 h. The precipitate formed was removed by centrifugation at 5000 rpm for 15 min. The absorbance was then measured at 280 nm using a spectrophotometer against a blank where TCA was added prior to the incubation period. Unit of enzymatic activity was defined as the amount of enzyme that produced products by breaking down casein giving an absorbance of 0.1 at 280 nm under the experimental conditions. The following formula was used to calculate the activity of protease per mg of protein.

$$\text{Protease activity (U/ mL)} = \text{OD (280 nm)}/(0.01 \times \text{Time} \times \text{volume}).$$

2.16. Statistical analysis

Statistical analysis of the data was carried out using a one-way analysis of variance (ANOVA) with Tukey's multiple comparison tests at a significance level of $p < 0.05$ using the SPSS 20 software (IBM, USA).

3. Results and discussion

3.1. Preparation and characterization of GF solid dispersions

In addition to improving dissolution and antifungal activity, presence of surfactants can affect the drug's physiochemical properties. Based on X-ray powder diffraction analysis, the formed crystals shape, volume and dimensions were not affected by the presence of surfactants (data not shown). The lattice parameters for GF showed tetragonal shaped crystals with values of a = 19.7 Å and c = 8.9 Å in agreement with previous studies [19–21]. Indexing of the observed peaks matched the peaks for GF, which reflected no polymorphic changes in the crystalline lattices when mixed with polymers and surfactants.

In agreement with XRPD results, the DSC thermographs indicated that when GF was present in the solid dispersion with or without the presence of a surfactant, it was present as semi-crystalline exhibiting a broad melting endotherm typically seen in milled solid materials (Fig. 1). The data indicates a variation in the relative amount of crystalline/amorphous content of the solid dispersions which was dependent upon the type, and, to a lesser extent, the amount of surfactant contained in the solid dispersion. For instance, in the cases of SDS-containing solid dispersions milled for two minutes, the crystalline content decreased from ~ 61 % for dispersions containing 1 wt% SDS to ~ 34 % for dispersions containing 5 wt% SDS. Consequently, the variation in the amount of amorphous content of the solid dispersions containing 1 wt% surfactant followed the order: solid dispersions containing SDS > solid dispersions with no surfactant > solid dispersions containing Pluronic F127 > solid dispersions containing DTAB. A similar trend was seen for the solid dispersions containing the higher ratios (i.e. 2.5 and 5 wt%) of surfactant, with the exception that the order was reversed for solid dispersions containing DTAB and Pluronic F127. The shift in the melting of GF when in the solid dispersion, compared to the pure drug, is indicative of the drug dissolving in the polymer network of the solid dispersion [22].

As a sign of altered molecular interactions upon mixing with the polymer, the glass transition temperature was found to change upon milling. As can be seen in Fig. 1, milled solid dispersions showed different T_g values where for example T_g decreased from ~ 364 K to around 356 K for milled solid dispersions containing F127. Similar trends could be observed where T_g seemed to be greatly influenced not only by the presence of the surfactant but also by the progressed mixing. Statistical analysis using ANOVA showed that the T_g values beyond 6–8 min milling were similar signifying that a minimum mechanical treatment exists where beyond this time, the particles seemed to have reached a constant T_g.

The broad nature of the melting endotherms may indicate the presence of different sizes of the particles leading to a lowering of the melting temperature and broadening of the melting endotherm. The polydisperse nature of the particles of the solid dispersion is supported by the results of the SEM study (Fig. 1). The broadening and lowering in the endotherm were more evident in the presence of surfactant. A slightly sharper melting endotherm was observed for surfactant containing particles, suggesting that these particles are less polydisperse in nature and therefore melt more uniformly.

The impact of longer milling times on the melting temperature was clear for all dispersions containing surfactants (Fig. 2). For SDS containing solid dispersions, equilibrium was observed after almost 2 min for all dispersions. For DTAB solid dispersions, equilibrium was reached after 8 min for 1 % DTAB solid dispersions. Faster equilibrium was reached for the 2.5 and 5 % DTAB solid dispersions reflecting the increased miscibility of the polymer/drug blends. For F127, solid dispersions, longer milling times were needed for the blends to reach the same melting temperature.

3.2. Saturated solubility and assessment of the formed nanosuspensions

The measurements of the apparent aqueous equilibrium solubility of GF obtained from the physical mixtures showed that incorporation of the anionic surfactant, SDS, into the physical mixture of GF:HPMCAS tended to increase the apparent equilibrium solubility of GF - solubility of GF in water was determined to be 40 μg/mL. Increasing the surfactant ratio (SDS or Pluronic F127) had minimal impact on the solubility of GF (range 115 to 125 μg/mL) while the presence of DTAB in the physical mixture actually resulted in a decrease in the apparent equilibrium solubility of GF. When comparing these results with the solubility of the drug from milled solid dispersions (Fig. 3), it was found that depending

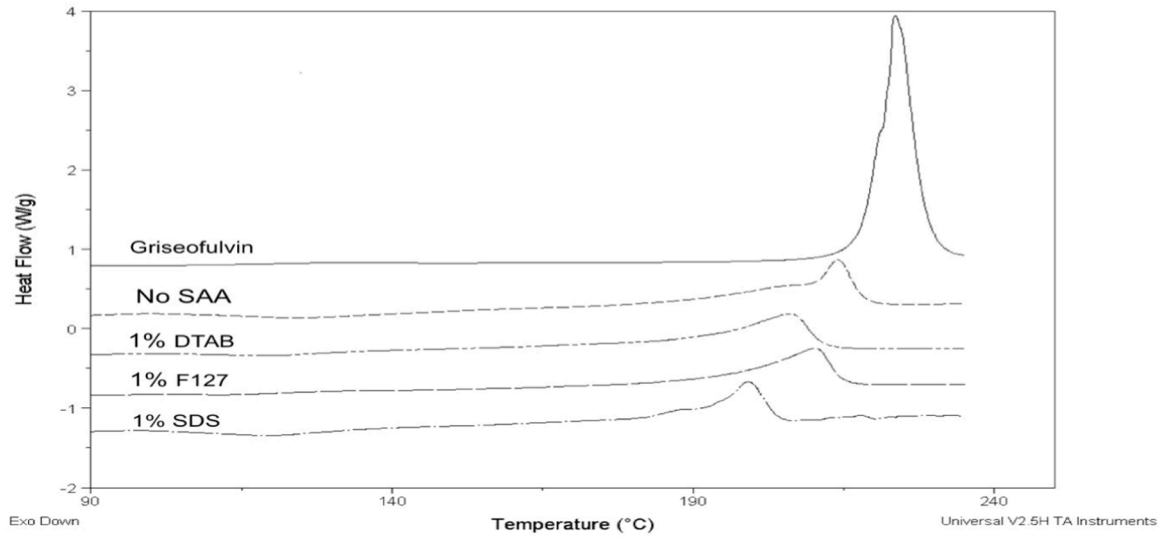

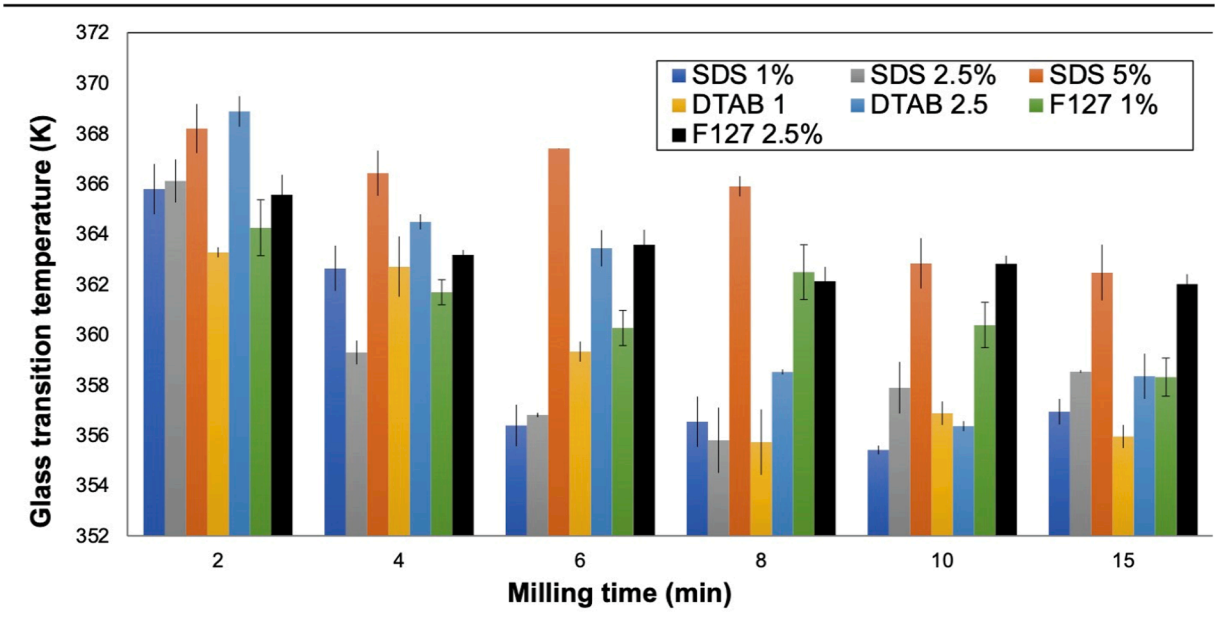

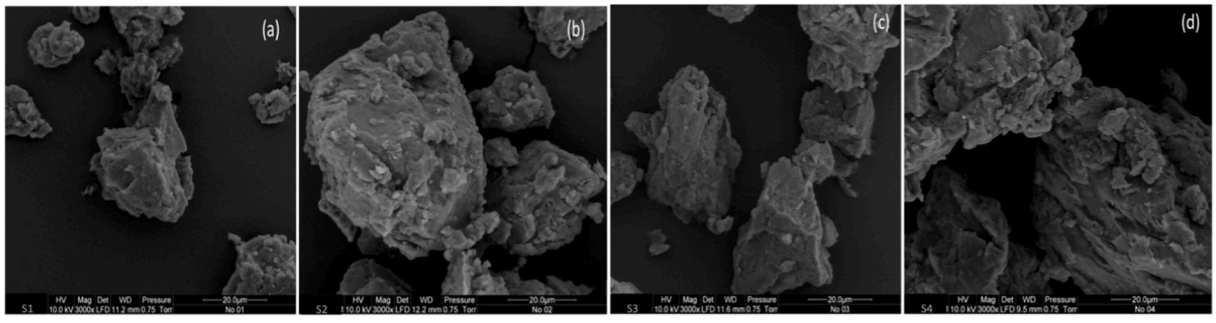

Fig. 1. (Top) differential scanning calorimetry thermograms of GF and 1:1 GF:HPMCAS milled solid dispersions containing 1 wt% SDS, 1 wt% DTAB, 1 wt% F127 and no surfactant; (Middle) Glass transition temperature (T_g) measurements as a function of different milling times used to prepare the milled solid dispersions of GF/HPMCAS, 1:1 and SDS, DTAB or F127; (Bottom) Scanning electron microscopy images of the GF:HPMCAS ball milled solid dispersions prepared using for 10 min milling and containing (a) 1 wt% SDS, (b) 1 wt% DTAB, (c) 1 wt% Pluronic F127 and (d) no surfactant.

upon the milling time used to prepare the solid dispersions; with an increase in ball milling time generally resulting in an increase in the apparent solubility of the GF. Milling time varied from 2 to 15 min resulted in increasing the apparent GF solubility from 240 to 800 μg/mL, with values reaching around 1200 μg/mL. However, as per physical mixtures increasing the ratio of the surfactant had a minimal impact on solubility. It was observed, however, that increasing DTAB ratio from 1 to 5 % had a dramatic negative impact on solubility with solubility decreased from 750 μg/mL to ~ 120 μg/mL.

The particle size of the nanosuspensions was investigated to

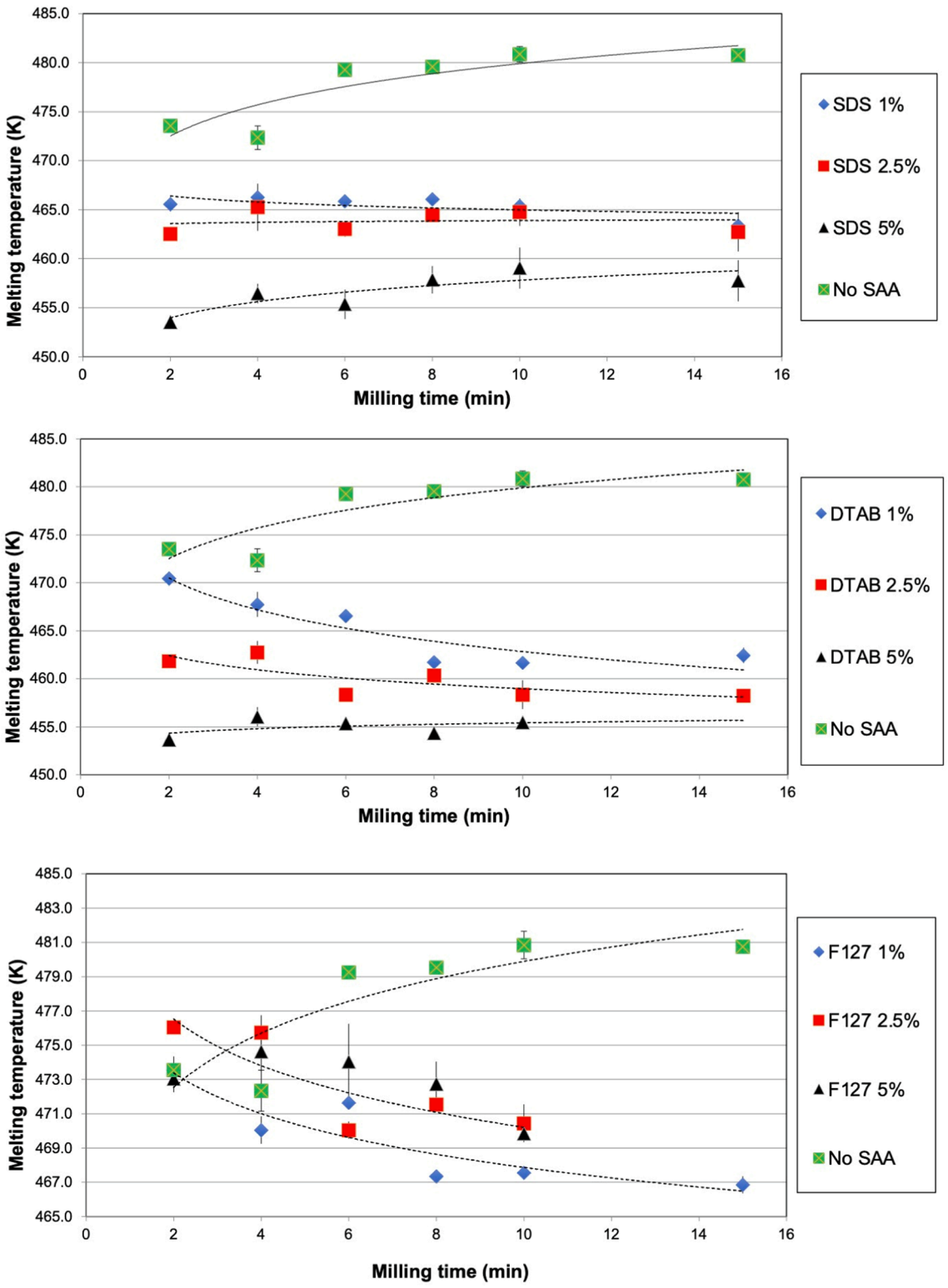

Fig. 2. Melting point onset in relation to milling time used to prepare milled solid dispersions of GF/HPMCAS, 1:1 and SDS, DTAB or F127.

determine stability and differences among different formulations. The size of the particles of the various nanosuspensions upon dispersal in an aqueous media of phosphate buffer at pH 6.8 was measured using laser diffraction (Fig. 4). While it is acknowledged that the sizes may not reflect the original size of the particles present in the parent solid dispersion, they can be used to assess whether the particles have aggregated/agglomerated in water. With this limitation in mind, it can be seen that the size of the surfactant-containing solid dispersions after two minutes in suspension exhibited a smaller size than the original (surfactant-free) solid dispersion. Furthermore, as the amount of surfactant used to prepare the solid dispersion increases, the size of the resultant particles of nanosuspensions decreased (Fig. 4). For example, upon dispersal, the particle size range measured of the SDS-containing particles was 4.9–15 μm for dispersions containing 1 wt% SDS and

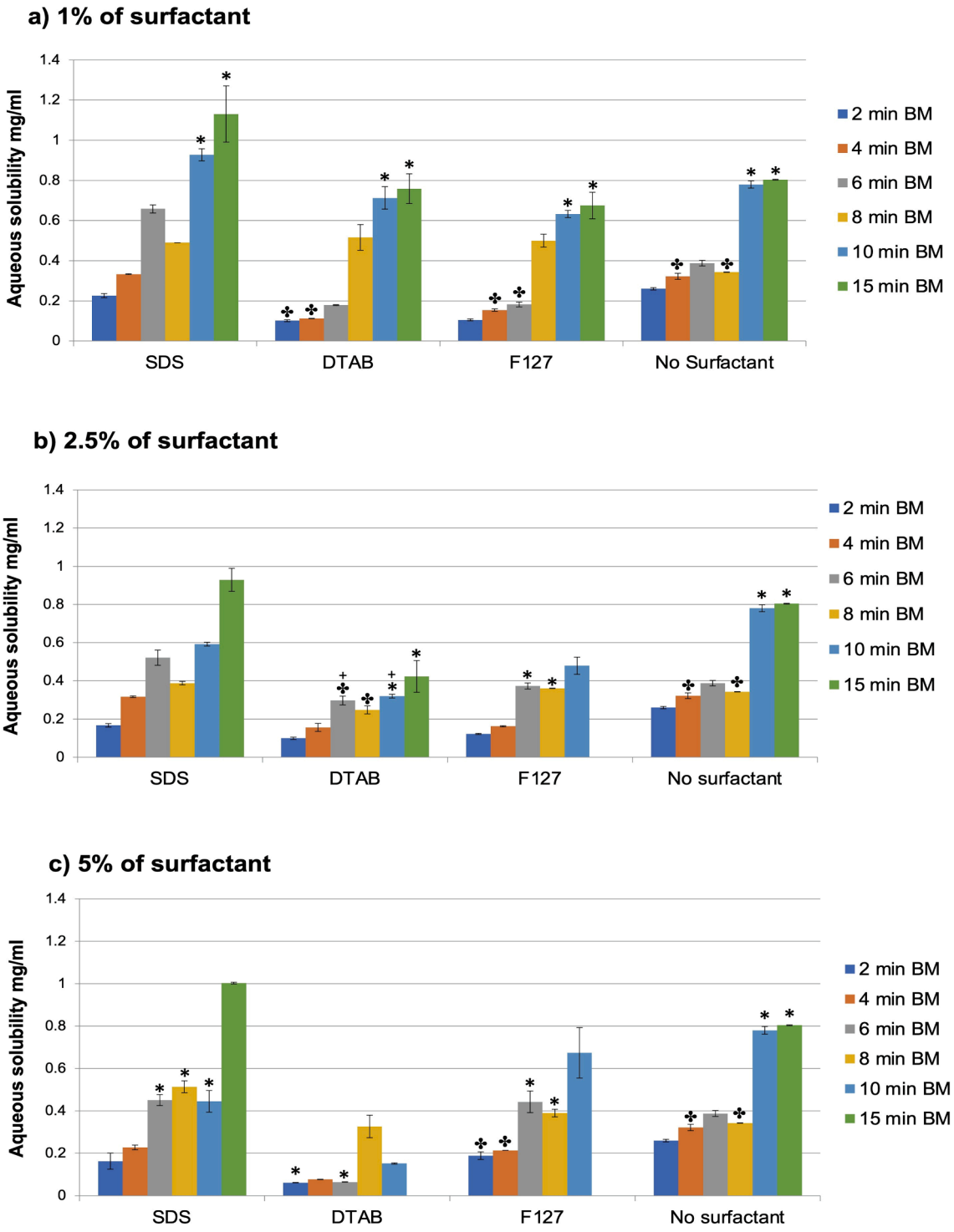

Fig. 3. Apparent saturation solubility of GF from ball milled solid dispersions containing a 1:1 wt ratio of GF:HPMCAS bead prepared by milling for differing periods and containing (a) 1 wt%, (b) 2.5 wt% or (c) 5 wt% surfactant (either SDS, DTAB or Pluronic F127). For comparison the results obtained for milled solid dispersion without surfactant are shown. All measurements were performed in triplicate and made using phosphate buffer at pH = 6.8 as solvent at room temperature. The symbols *, + indicate no statistical difference among annotated groups, the rest of data sets are statistically different ($p < 0.05$). All measurements were repeated in triplicate, the data represent mean ± SD.

4.8–7.8 μm for dispersions prepared using 5 wt% SDS. A similar, but more pronounced reduction in size range upon increasing surfactant was observed for the nanosuspensions containing DTAB and Pluronic F127 where the size decreased from 14 to 38 to 4.5–6 μm upon increasing DTAB ratio from 1 to 5 wt% and from 8.6 to 25 to 3.6–6.4 μm in going from 1 to 5 wt% Pluronic F127. The nanosuspensions prepared using 1 wt% SDS were smaller in size than those containing the same amount of either DTAB or Pluronic F127, a similar result to that seen with the SEM measurements of solid dispersions containing 1 wt% of surfactant. In contrast, however, the size of the nanosuspensions containing 5 wt% surfactant was of a much more comparable size and independent of surfactant type.

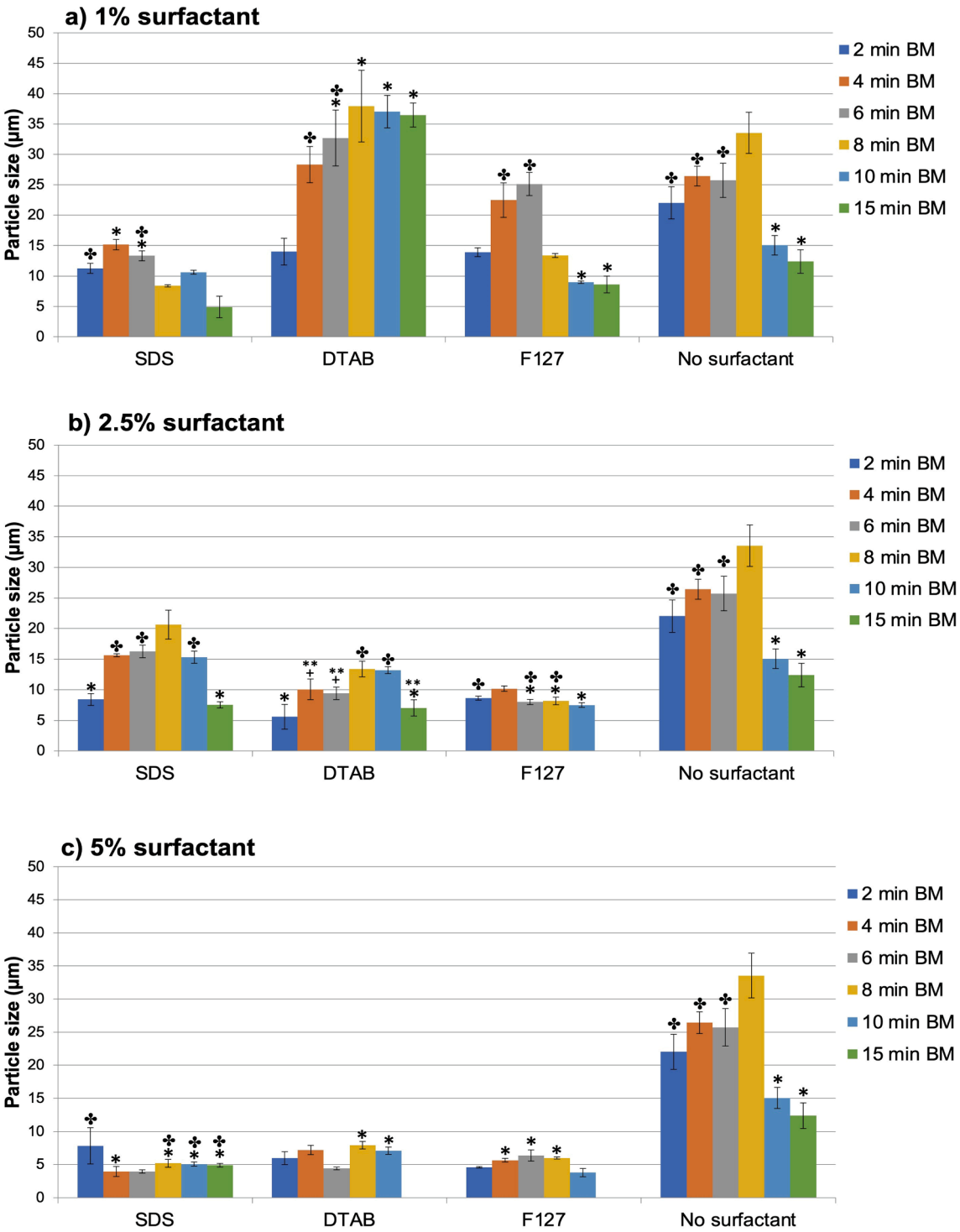

Fig. 4. Particle size analysis of GF nanosuspensions prepared from ball milled solid dispersions containing a 1:1 wt ratio of GF:HPMCAS bead prepared by milling for differing periods and containing (a) 1 wt%, (b) 2.5 wt% or (c) 5 wt% surfactant (either SDS, DTAB or Pluronic F127). For comparison the results obtained for milled solid dispersion without surfactant are shown. All measurements were performed in triplicate and made using phosphate buffer at pH = 6.8 as solvent at room temperature. The symbols *, **, ✤, + indicate no statistical difference among annotated groups, the rest of data sets are statistically different ($p < 0.05$). All measurements were repeated in triplicate, the data represent mean ± SD.

3.3. Assessment of sorption/ desorption using dynamic vapor sorption (DVS)

It is essential for the drug formulation to adhere to the surface of the nail otherwise minimal absorption of the drug would occur. The potential to adhere to the surface is related to the extent and rate of water uptake which was assessed using dynamic vapor sorption (DVS). Within a typical measurement, the sample undergoes a reversible sorption/ desorption event. The result is sorption isotherm which describes the amount of water (vapor) adsorbed or desorbed at the surface at different partial pressures. The isotherm shapes can identify the nature of the material and in general materials are classified according to their isotherm based on the BDDT classification [23].

It Is generally agreed that adsorption of water can occur through

either monolayer formation, cluster formation or combination. If the heat of sorption is high (i.e., high affinity of vapour to adsorb to the surface) then the water molecules will adsorb as a monolayer of molecules. On the contrary if the heat of sorption was similar to the heat of condensation, only small number of molecules will adsorb at the surface at low partial pressures. This results in condensation at higher partial pressures and therefore cluster formation as opposed to monolayer formation. For mixtures such as the studied solid dispersions, a type IV hysteresis is expected which implicates that cluster formation would occur.

As can be seen in Fig. 5, adsorption did not coincide with the desorption indicating different kinetics for water removal. This hysteresis (i.e. difference between the two events) can explain how the material responds to water activity. Upon inclusion of surfactants into the GF: HMCAS solid dispersion the hysteresis shape did not change but rather the total amount of adsorbed water has increased. When comparing the different surfactants, SDS and DTAB exhibited similar pattern showing reduced absorption at partial pressure of approximately below 70 %. On the contrary SDS and DTAB showed slightly higher hydrophilicity especially at partial pressure above 70 %. In the case of SDS and DTAB solid dispersions, longer milling time led to enhanced amount of absorption but again the hysteresis has not changed. Interestingly, F127 solid dispersions did not show any change in the isotherm even when milled for 10 min. This differences in the hysteresis upon changing the surfactant type and milling conditions indicate that the surface/bulk properties have changed, and these changes are dependent on milling conditions.

3.4. Assessment of permeability using Raman mapping

In this study bovine hooves were used as model for the human nail. To assess permeability, Raman mapping was used as opposed to other methods used in the literature. Rationale to use Raman mapping is the ability to distinguish the drug from other components but more importantly is the simulation of real conditions that are used when the formulation was to be applied by the patient. The analytical benefit for this technique is that the drug can be differentiated from the hoof tissue. The sliced bovine hooves were immersed into the nanosuspensions and then removed and dried. Any residual powder was removed to ensure that the measured spectra reflect drug that penetrated through the tissue. The amount of GF that that was applied was identical (approximately 1 % w/v) so that to ensure no differences result from larger or lower amounts of GF applied on the hoof. For each formulation, 10 mg of GF suspended in 1 mL denoised water or ethanol were applied to each sample and each was repeated in triplicate to ensure reproducible data. We also verified similar patterns by scanning different regions within the same hoof sample.

Analysis of Raman data (Fig. 6) revealed presence of GF in all hoof samples except hoof soaked in ethanol which acted as a control. Formulations in order of most to least GF distribution are as follows: DTAB > F127 > No Surfactant > SDS. Formulations in order of highest to lowest GF concentration are as follows: DTAB > F127 > SDS > No Surfactant. Amount of GF was estimated based on intensity of identifiable peaks at ~ 1600 and ~ 1700 cm^{-1}. This is demonstrated in Fig. 6 by a spectrum from a single point on each Raman map (red) showing highest intensity of GF compared to GF reference (blue). From these results it can be concluded that adding a polymer to the GF formulations enhanced the surface adherence the bovine hoof. Furthermore, the addition of a surfactant increased the penetration of GF dependant on the type of surfactant used. GF is likely to have adhered to the hoof surface rather than formed a film coating as this would have been removed during the hoof cleaning step. It is difficult to draw conclusions from GF peak intensity within the map as these may be influenced by the Raman laser focusing. Since the hoof samples were not completely flat, and auto focusing was not available, poor focusing may account for the differences seen (for example between SDS and no Surfactant).

3.5. Assessment of antifungal activity on infected bovine hooves

The validity of infected slices of bovine hooves to study the effect of drugs was demonstrated elsewhere [24]. The hooves were sliced to a similar thickness so that to mimic human nail of approximately 300 μm. The results showed a higher level of *T. rubrum* NCPF 935 biofilm inhibition was achieved with F6, F8 and F9 formulations containing GF

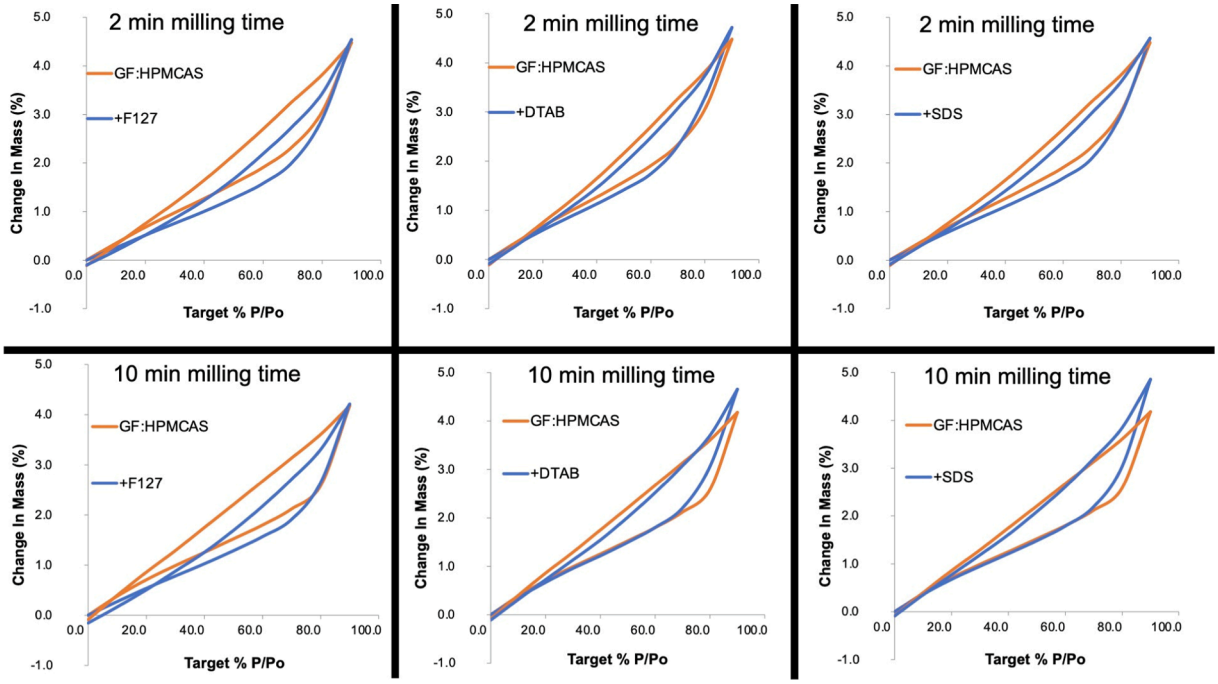

Fig. 5. Dynamic vapour sorption (DVS) of ball milled solid dispersions containing a 1:1 wt ratio of GF:HPMCAS bead prepared by milling for 2 and 10 min and containing 2.5 wt% surfactant (either SDS, DTAB or Pluronic F127). For comparison the results obtained for milled solid dispersion without surfactant are shown.

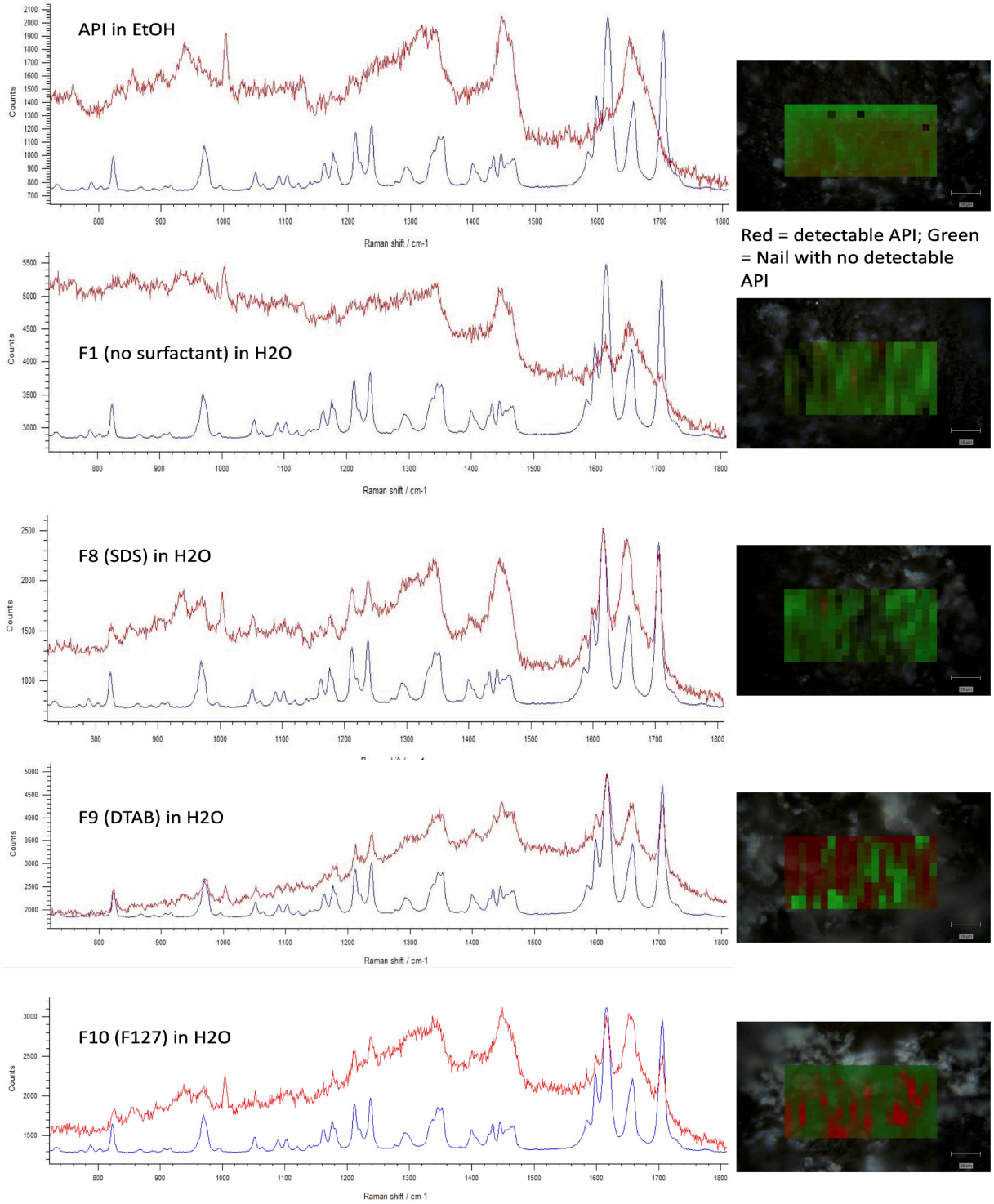

Fig. 6. Raman mapping data of bovine hoof (nail) exposed to GF in ethanol, no surfactant in water, SDS in water, DTAB in water and F127 in water (surfactant ratio is 2.5 %). Red = detectable API; Green = Nail with no detectable. API Spectra = a single datapoint from red region of the map where programme detected API. No API detectable for ethanol map. The blue spectra refer to drug and the red spectra refer to formulations on hooves. (For interpretation of the references to colour in this figure legend, the reader is referred to the web version of this article.)

(Fig. 7). The effect of F6, F8 and F9 were further observed to reduce the ECM content of *T. rubrum* NCPF 935 biofilm compared to the other formulations. However, F9 seemed to be the most effective of all in reducing ECM content of the biofilm. The difference was statistically significant when compared to other formulations. Of the three formulations, F8 and F9 were found to be the most effective in reducing the metabolic activity of *T. rubrum* NCPF 935 over a period of 96 h, when compared to F6 as well as the untreated control ($p < 0.05$). The reduction in the metabolic activity was apparent after a period of 48 hr till the end of the experiment. Similarly, F6 and F9 were found to show the highest reduction in protease production which is a common enzymatic virulence factor produced by saprophytic fungi. However, statistical difference was only significant when compared with F6, F12 and F13. These results showed that formulations containing GF: HPMCAS (1:1)

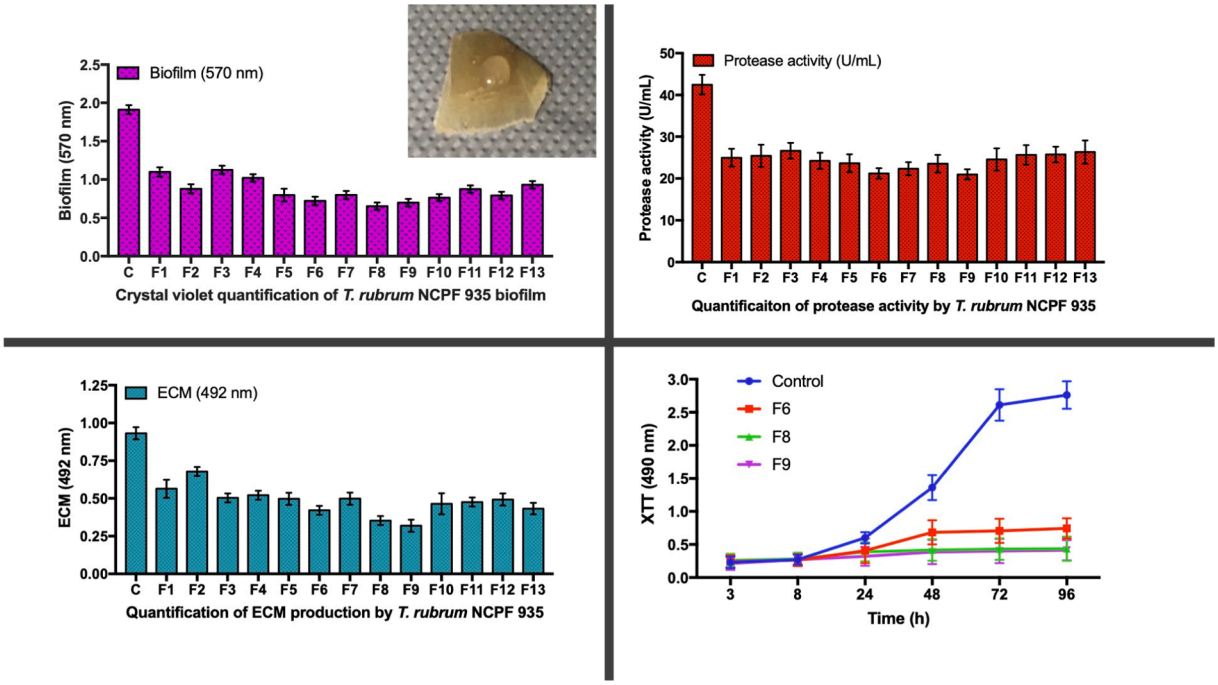

Fig. 7. Assessment of antifungal activity on infected bovine hoof showing effect on biofilm activity, protease activity, ECM production and XTT analysis. All measurements were repeated in triplicate, the data represent mean ± SD (detailed statistical analysis can be found in appendix). The inset shows hoof slice with a drop of the nanosuspension.

along with DATB (2.5 % and 5 %) were highly effective against biofilm formation by *T. rubrum*. Similarly, GF: HPMCAS + 2.5 % SDS was found to be substantially potent when compared with all the 13 formulations used in this study. Inclusion of colloidal silver did not seem to improve antifungal activity as compared with other formulations.

F1: GF (49.5 %): HPMCAS (49.5 %) + 1 % Ag;
F2: GF (47 %): HPMCAS (47 %) + 1 % Ag + 5 % SDS;
F3: GF (47 %): HPMCAS (47 %) + 1 % Ag + 5 % DTAB;
F4: GF (47 %): HPMCAS (47 %) + 1 % Ag + 5 % Pluronic F127;
F5: GF (47.5 %): HPMCAS (47.5 %) + 5 % SDS;
F6: GF (47.5 %): HPMCAS (47.5 %) + 5 % DTAB;
F7: GF (47.5 %): HPMCAS (47.5 %) + 5 % PluronicF127;
F8: GF (48.75 %): HPMCAS (48.75 %) + 2.5 % SDS;
F9: GF (48.75 %): HPMCAS (48.75 %) + 2.5 % DTAB;
F10: GF (48.75 %): HPMCAS (48.75 %) + 2.5 % PluronicF127;
F11: GF (49.5 %): HPMCAS (49.5 %) + 1 % SDS;
F12: GF (49.5 %): HPMCAS (49.5 %) + 1 % DTAB;
F13: GF (49.5 %): HPMCAS (49.5 %) + 1 % PluronicF127.

4. Conclusions

Solid dispersions of the antifungal drug griseofulvin were prepared by mechanochemical activation followed by formation of stable nanosuspensions. These formulations eliminate the need for organic solvents to help with solubilising the components as drug solubility was enhanced by the molecular mixing in solid state as well as inclusion of the surfactants. The results showed enhanced permeability through the bovine hooves. Inclusion of silver did not enhance the antifungal activity of the drug hence there is minimum benefit for its inclusion. Solid dispersions that contained DTAB showed optimum antifungal properties, and these can be suggested as potential formulations for onychomycosis.

Declaration of Competing Interest

The authors declare that they have no known competing financial interests or personal relationships that could have appeared to influence the work reported in this paper.

Data availability

Data will be made available on request.

Acknowledgements

The authors would like to thank the Chemical Analysis Facility at the University of Reading for providing essential access to instruments used in this study.

Appendix A. Supplementary material

Supplementary data to this article can be found online at https://doi.org/10.1016/j.ejpb.2022.09.004.

References

[1] B.E. Elewski, Onychomycosis: pathogenesis, diagnosis, and management, Clin. Microbiol. Rev. 11 (1998) 415–429.
[2] A.K. Gupta, S.G. Versteeg, N.H. Shear, Onychomycosis in the 21st Century: An Update on Diagnosis, Epidemiology, and Treatment, J. Cutan Med. Surg. 21 (6) (2017) 525–539.
[3] A.K. Gupta, K.A. Foley, Evidence for biofilms in onychomycosis, G Ital Dermatol. Venereol. 154 (2019) 50–55.
[4] K.F. Mitchell, R. Zarnowski, D.R. Andes, The extracellular matrix of fungal biofilms, Adv. Exp. Med. Biol. 931 (2016) 21–35.
[5] N. Høiby, T. Bjarnsholt, C. Moser, G.L. Bassi, T. Coenye, G. Donelli, L. Hall-Stoodley, V. Holá, C. Imbert, K. Kirketerp-Møller, D. Lebeaux, A. Oliver, A. J. Ullmann, C. Williams, ESCMID* guideline for the diagnosis and treatment of biofilm infections 2014, Clin. Microbiol. Infect. 21 (2015) S1–S25.
[6] N. Toukabri, S. Corpologno, M.E. Bougnoux, D. El Euch, N. Sadfi-Zouaoui, G. Simonetti, In vitro biofilms and antifungal susceptibility of dermatophyte and non-dermatophyte moulds involved in foot mycosis, Mycoses 61 (2018) 79–87.
[7] H. Al-Obaidi, M. Majumder, F. Bari, Amorphous and crystalline particulates: challenges and perspectives in drug delivery, Curr. Pharm. Des. 23 (2017) 350–361.
[8] H. Al-Obaidi, M.J. Lawrence, G. Buckton, Atypical effects of incorporated surfactants on stability and dissolution properties of amorphous polymeric dispersions, J. Pharm. Pharmacol. 68 (2016) 1373–1383.

[9] H. Al-Obaidi, R.M. Kowalczyk, R. Kalgudi, M.G. Zariwala, Griseofulvin solvate solid dispersions with synergistic effect against fungal biofilms, Colloids Surf B Biointerfaces 184 (2019), 110540.
[10] A. Bhanderi, F. Bari, H. Al-Obaidi, Evaluation of the impact of surfactants on miscibility of griseofulvin in spray dried amorphous solid dispersions, J. Drug Delivery Sci. Technol. 64 (2021), 102606.
[11] M. Simões, L.C. Simões, I. Machado, M.O. Pereira, M.J. Vieira, Control of flow-generated biofilms with surfactants: evidence of resistance and recovery, Food Bioprod. Process. 84 (4) (2006) 338–345.
[12] G. Czernel, D. Bloch, A. Matwijczuk, J. Cieśla, M. Kędzierska-Matysek, M. Florek, M. Gagoś, Biodirected Synthesis of Silver Nanoparticles Using Aqueous Honey Solutions and Evaluation of Their Antifungal Activity against Pathogenic Candida Spp, Int. J. Mol. Sci. 22 (14) (2021) 7715.
[13] A. Panacek, M. Kolar, R. Vecerova, R. Prucek, J. Soukupova, V. Krystof, P. Hamal, R. Zboril, L. Kvitek, Antifungal activity of silver nanoparticles against Candida spp, Biomaterials 30 (2009) 6333–6340.
[14] M. Robles-Martinez, J.F.C. Gonzalez, F.J. Perez-Vazquez, J.M. Montejano-Carrizales, E. Perez, R. Patino-Herrera, Antimycotic Activity Potentiation of Allium sativum Extract and Silver Nanoparticles against Trichophyton rubrum, Chem. Biodivers. 16 (2019) e1800525.
[15] L. Pereira, N. Dias, J. Carvalho, S. Fernandes, C. Santos, N. Lima, Synthesis, characterization and antifungal activity of chemically and fungal-produced silver nanoparticles against Trichophyton rubrum, J. Appl. Microbiol. 117 (2014) 1601–1613.
[16] M.E. Amin, M.M. Azab, A.M. Hanora, S. Abdalla, Antifungal activity of silver nanoparticles on Fluconazole resistant Dermatophytes identified by (GACA)4 and isolated from primary school children suffering from Tinea Capitis in Ismailia - Egypt, Cell Mol. Biol. (Noisy-le-grand) 63 (2017) 63–67.
[17] M. Aldén, M. Lydén, J. Tegenfeldt, Effect of counterions on the interactions in solid dispersions between polyethylene glycol, griseofulvin and alkali dodecyl sulphates, Int. J. Pharm. 110 (3) (1994) 267–276.
[18] H. Al-Obaidi, R. Kalgudi, M.G. Zariwala, Fabrication of inhaled hybrid silver/ciprofloxacin nanoparticles with synergetic effect against Pseudomonas aeruginosa, Eur. J. Pharm. Biopharm. 128 (2018) 27–35.
[19] K.C. Cheng, E. Shefter, T. Srikrishnan, Crystal-structure analysis of the desolvation of the chloroform solvate of Griseofulvin, Int. J. Pharm. 2 (2) (1979) 81–89.
[20] Puttaraja, K.A. Nirmala, D.S. Sakegowda, W.L. Duax, Crystal-structure of Griseofulvin, J. Crystallogr. Spectrosc. Res. 12 (5) (1982) 415–423.
[21] Q.Q. Pan, P. Guo, J. Duan, Q. Cheng, H. Li, Comparative crystal structure determination of griseofulvin: Powder X-ray diffraction versus single-crystal X-ray diffraction, Chin. Sci. Bull. 57 (2012) 3867–3871.
[22] S. Thakral, N.K. Thakral, Prediction of drug-polymer miscibility through the use of solubility parameter based flory-huggins interaction parameter and the experimental validation: PEG as model polymer, J. Pharm. Sci. 102 (2013) 2254–2263.
[23] S. Brunauer, L.S. Deming, W.E. Deming, E. Teller, On a theory of the van der Waals adsorption of gases, J. Am. Chem. Soc. 62 (1940) 1723–1732.
[24] D. Monti, L. Saccomani, P. Chetoni, S. Burgalassi, S. Tampucci, F. Mailland, Validation of bovine hoof slices as a model for infected human toenails: in vitro ciclopirox transungual permeation, Br. J. Dermatol. 165 (2011) 99–105.